Stepwise Reactions of Acetylenes with Iridium Thiocarbonyl Complexes To Produce Isolable Iridacyclobutadienes and Conversion of These to either Cyclopentadienyliridium or Tethered Iridabenzene Complexes

George R. Clark, Guo-Liang Lu, Warren R. Roper,* and L. James Wright*

Department of Chemistry, The University of Auckland, Private Bag 92019, Auckland, New Zealand

Received November 20, 2006

Treatment of $IrCl(CS)(PPh_3)_2$ with an excess of KI gives orange $IrI(CS)(PPh_3)_2$ (**1**). $IrI(CS)(PPh_3)_2$ (**1**) reacts reversibly with dioxygen to form the brown dioxygen complex $Ir(O_2)I(CS)(PPh_3)_2$ (**2**). Reaction between $IrI(CS)(PPh_3)_2$ (**1**) and 2 equiv of ethyne produces the green-brown tethered iridacyclobutadiene complex $Ir[C_3H_2(CH{=}CHS\text{-}1)]I(PPh_3)_2$ (**3**), one ethyne combining in a cycloaddition reaction with the IrC multiple bond to the CS ligand to form the four-membered IrC_3 ring and the second ethyne alkylating the sulfur atom to give the vinylthio substituent at the 1-position of the metallacyclic ring, which is tethered to the iridium through an Ir−C bond. In reactions related to those with ethyne, phenylacetylene reacts with $IrCl(CS)(PPh_3)_2$ to give as the major product the tethered iridacyclobutadiene $Ir[C_3H(CH{=}C\{Ph\}S\text{-}1)(Ph\text{-}3)]Cl(PPh_3)_2$ (**4**), with the phenyl substituent adjacent to the iridium, and as the minor product the isomeric tethered iridacyclobutadiene $Ir[C_3H(CH{=}C\{Ph\}S\text{-}1)(Ph\text{-}2)]Cl(PPh_3)_2$ (**5**). A thermal reaction of $Ir[C_3H(CH{=}C\{Ph\}S\text{-}1)(Ph\text{-}3)]Cl(PPh_3)_2$ (**4**) with further phenylacetylene produces the tethered, substituted cyclopentadienyliridium complex $Ir[\eta^5\text{-}C_5H_2(SCPh{=}CH\text{-}1)(Ph\text{-}3)(Ph\text{-}5)]Cl(PPh_3)$ (**6**), which retains the iridium−carbon bond to the vinylthio substituent. Methyl propiolate reacts with $IrI(CS)(PPh_3)_2$ (**1**) to form exclusively the tethered iridacyclobutadiene $Ir[C_3H(CH{=}C\{CO_2Me\}S\text{-}1)(CO_2Me\text{-}2)]I(PPh_3)_2$ (**7**). Treatment of this iridacyclobutadiene, **7**, with silver triflate allows introduction of a third methyl propiolate, which brings about ring expansion of the iridacyclobutadiene to form the stable tethered iridabenzene $Ir[C_5H_2(CH{=}C\{CO_2Me\}S\text{-}1)(CO_2Me\text{-}2)(CO_2Me\text{-}4)]Cl(PPh_3)_2$ (**8**). Complex **8** retains the same vinylthio tethering group as found in **7**. The structures of **2**−**8** have been confirmed by X-ray crystal structure determinations. Both NMR spectroscopic and structural data for **8** support the formulation of this compound as a tethered metallaaromatic molecule.

Introduction

In the first metallabenzene synthesis, the OsC_5 ring of the osmabenzene was assembled from two ethyne molecules and the single carbon atom from a thiocarbonyl ligand already resident on the osmium in the starting material, $Os(CS)(CO)(PPh_3)_3$.[1] An intriguing possibility is that other low-oxidation-state transition-metal thiocarbonyl complexes might also provide a simple route into metallabenzene systems, through reactions with acetylenes; however, this has not yet been adequately explored. We address this question in this paper by examining reactions between neutral iridium thiocarbonyl complexes and several acetylenes.

A computational study of the formation of the original osmabenzene, $Os[C_5H_4(S\text{-}1)](CO)(PPh_3)_2$,[2] considered two distinct pathways. The first step in both pathways involves coordination of one ethyne to the metal, producing intermediate **A** in Scheme 1. According to the computational results,[2] the next step in the more favorable pathway is formation of an osmacyclobutenethione ring (intermediate **B**) from combination of CS with the ethyne molecule, followed by ring expansion through reaction with a second ethyne to give an osmacyclohexadienethione (intermediate **C**) and finally aromatization of this osmacyclohexadienethione through coordination of sulfur to osmium to give osmabenzene **D**. In practice, osmabenzene **D** proved to alkylate readily at sulfur to give osmabenzene **E**.[1] There are experimental precedents for intermediate **A** $(Os(CS)(PhC_2Ph)(PPh_3)_2)$,[3] intermediate **B** $(Os[C_3(S\text{-}1)(Ph\text{-}2)(Ph\text{-}3)](CO)_2(PPh_3)_2)$,[3] and intermediate **C** $(Os[C_5H_4(S\text{-}1)](CO)_2(PPh_3)_2)$.[1] The less favorable pathway, according to the computational results, involves initial formation of an osmacyclopentadiene (intermediate **G**) from combination of one further ethyne molecule with intermediate **A**, followed ultimately

Scheme 1

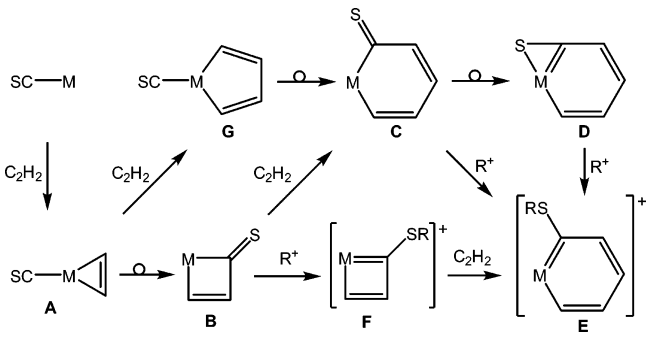

(1) Elliott, G. P.; Roper, W. R.; Waters, J. M. *J. Chem. Soc., Chem. Commun.* **1982**, 811.

(2) Iron, M. A.; Lucassen, A. C. B.; Cohen, H.; van der Boom, M. E.; Martin, J. M. L. *J. Am. Chem. Soc*. **2004**, *126*, 11699.

(3) (a) Elliott, G. P.; Roper, W. R. *J. Organomet. Chem.* **1983**, *250*, C5. (b) Burrell, A. K.; Elliott, G. P.; Rickard, C. E. F.; Roper, W. R. *Appl. Organomet. Chem.* **1990**, *4*, 535.

10.1021/om061066r CCC: $37.00
Publication on Web 03/27/2007

Scheme 2

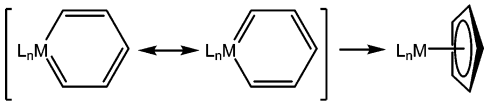

by ring expansion through insertion of the thiocarbonyl ligand into this five-membered ring to give **C**. Either pathway depends for its success on the readiness with which the thiocarbonyl ligand undergoes insertion reactions. In related work we have demonstrated that the thiocarbonyl ligand will insert into Os−H,[4] Os−C,[5] Os−Si,[6] and Os−B[7] bonds. With the exception of the Os−C bond, insertion of the related carbonyl ligand into these bonds has not been observed.

A variant of the favored route, **A** to **B** to **C** to **D**, involves an electrophile intercepting **B** and effecting S-alkylation to give the metallacyclobutadiene complex **F**. Metallacyclobutadiene complexes are well-characterized species and have been proposed as key intermediates in metal-catalyzed alkyne metathesis reactions.[8] Some metallacyclobutadiene complexes react with acetylenes to form metal cyclopentadienyl complexes. This reaction has been proposed to proceed through metallabenzene intermediates[9] and has also been suggested as a route for catalyst deactivation in metal-catalyzed alkyne metathesis.[8] Computational studies have shown that many metallabenzene complexes can readily rearrange to cyclopentadienyl complexes (see Scheme 2).[10] As far as we are aware, no direct conversion of a stable metallacyclobutadiene complex to a stable metallabenzene complex through ring expansion with an acetylene, i.e., conversion of **F** to **E** in Scheme 1, has been reported.

In this paper we report (i) the formation of the thiocarbonyl complex $IrI(CS)(PPh_3)_2$ (**1**) and the structural characterization of the dioxygen adduct $Ir(O_2)I(CS)(PPh_3)_2$ (**2**), (ii) the reaction of $IrI(CS)(PPh_3)_2$ (**1**) with ethyne to form the tethered iridacyclobutadiene complex $Ir[C_3H_2(CH{=}CHS\text{-}1)]I(PPh_3)_2$ (**3**), (iii) the reaction of $IrCl(CS)(PPh_3)_2$ with phenylacetylene to form the isomeric tethered iridacyclobutadienes $Ir[C_3H(CH{=}C\{Ph\}S\text{-}1)(Ph\text{-}3)]Cl(PPh_3)_2$ (**4**) and $Ir[C_3H(CH{=}C\{Ph\}S\text{-}1)(Ph\text{-}2)]Cl(PPh_3)_2$, (iv) the thermal reaction of $Ir[C_3H(CH{=}C\{Ph\}S\text{-}1)(Ph\text{-}3)]Cl(PPh_3)_2$ (**4**) with further phenylacetylene to produce the tethered, substituted cyclopentadienyliridium complex $Ir[\eta^5\text{-}C_5H_2(SCPh{=}CH\text{-}1)(Ph\text{-}3)(Ph\text{-}5)]Cl(PPh_3)$ (**6**), (v) the reaction of $IrI(CS)(PPh_3)_2$ (**1**) with methyl propiolate to give the tethered iridayclobutadiene $Ir[C_3H(CH{=}C\{CO_2Me\}S\text{-}1)(CO_2Me\text{-}2)]I(PPh_3)_2$ (**7**), (vi) the reaction of $Ir[C_3H(CH{=}C\{CO_2Me\}S\text{-}1)(CO_2Me\text{-}2)]I(PPh_3)_2$ (**7**) with silver triflate followed by methyl propiolate to bring about ring expansion of the iridacyclobutadiene to form the tethered iridabenzene $Ir[C_5H_2(CH{=}C\{CO_2Me\}S\text{-}1)(CO_2Me\text{-}2)(CO_2Me\text{-}4)]Cl(PPh_3)_2$ (**8**), and (vii) the crystal structures of **2**−**8**.

Scheme 3

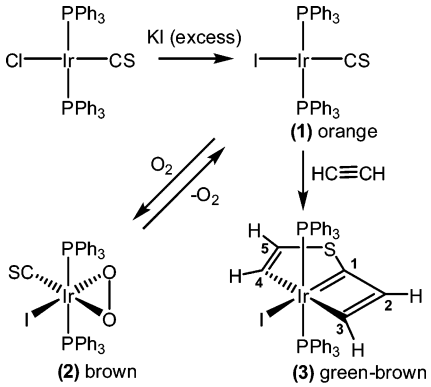

Results and Discussion

Preparation of $IrI(CS)(PPh_3)_2$ (1), the Reversible Reaction of This Compound with Dioxygen To Form $Ir(O_2)I(CS)(PPh_3)_2$ (2), and the Crystal Structure of 2. For the carbonyl complexes $IrX(CO)(PPh_3)_2$ it is well-established that the reactivity of individual compounds toward oxidative addition reactions is dependent upon the nature of the anionic ligand X: e.g., for $IrCl(CO)(PPh_3)_2$ dioxygen uptake is reversible, whereas for $IrI(CO)(PPh_3)_2$ dioxygen uptake is irreversible.[11] The thiocarbonyl complex $IrCl(CS)(PPh_3)_2$ is not particularly soluble in chlorinated solvents, and anticipating both greater solubility and enhanced reactivity of the iodo analogue $IrI(CS)(PPh_3)_2$, we chose to examine the reactivity of both compounds toward acetylenes.

As illustrated in Scheme 3 (carbon atoms are numbered for NMR discussion), treatment of $IrCl(CS)(PPh_3)_2$ with an excess of potassium iodide effectively produces orange $IrI(CS)(PPh_3)_2$ (**1**) in high yield. In the IR spectrum of **1** ν(CS) appears as a strong band at 1322 cm^{-1}, and in the ^{31}P NMR spectrum there is a singlet resonance at 24.36 ppm arising from the two equivalent, mutually trans PPh_3 ligands. Orange solutions of **1** become brown on exposure to air, with formation of the brown dioxygen adduct $Ir(O_2)I(CS)(PPh_3)_2$ (**2**). This dioxygen uptake could be reversed on heating solutions of **2** under vacuum. In the IR spectrum of **2** $\nu(Ir{-}O_2)$ is observed as a band of medium intensity at 858 cm^{-1}. This can be compared with the reported values of 858 cm^{-1} for $Ir(O_2)Cl(CO)(PPh_3)_2$ and 862 cm^{-1} for $Ir(O_2)I(CO)(PPh_3)_2$.[11] Although the ν(CS) band for **2** at 1321 cm^{-1} is not changed significantly from that of the parent compound (ν(CS) values typically are less responsive to any molecular change than is ν(CO) and occur in a narrower range), in the ^{31}P NMR spectrum the two equivalent, mutually trans PPh_3 ligands appear as a singlet resonance at the considerably upfield position of 5.19 ppm. Both **1** and **2** have good solubility in benzene and chlorinated solvents. Furthermore, the reversible dioxygen uptake allowed samples of $IrI(CS)(PPh_3)_2$ (**1**) containing variable quantities of $Ir(O_2)I(CS)(PPh_3)_2$ (**2**) to be used in reactions with acetylenes without adversely affecting the overall yield.

The crystal structure of $Ir(O_2)I(CS)(PPh_3)_2$ (**2**) was determined, and the molecular structure is shown in Figure 1. The crystal data and refinement details for **2** and for the other crystal structures reported in this paper are collected in Table 1. Selected bond lengths and angles for **2** are presented in Table 2. The geometry of **2** is closely similar to that of the carbonyl analogue $Ir(O_2)I(CO)(PPh_3)_2$. However, the measured O−O distance at

(4) (a) Collins, T. J.; Roper, W. R. *J. Chem. Soc., Chem. Commun.* **1976**, 1044. (b) Roper, W. R.; Town, K. G. *J. Chem. Soc., Chem. Commun.* **1977**, 781.

(5) Clark, G. R.; Collins, T. J.; Marsden, K.; Roper, W. R. *J. Organomet. Chem.* **1978**, *157*, C23.

(6) Rickard, C. E. F.; Roper, W. R.; Salter, D. M.; Wright, L. J. *Organometallics* **1992**, *11*, 3931.

(7) Irvine, G. J.; Lesley, M. J. G.; Marder, T. B.; Norman, N. C.; Rice, C. R.; Robins, E. G.; Roper, W. R.; Whittell, G. R.; Wright, L. J. *Chem. Rev.* **1998**, *98*, 2685.

(8) (a) Schrock, R. R.; Pedersen, S. F.; Churchill, M. R.; Ziller, J. W. *Organometallics* **1984**, *3*, 1574. (b) Zhu, J.; Jia, G.; Lin, Z. *Organometallics* **2006**, *25*, 1812.

(9) (a) Plantevin, V.; Wojcicki, A. *J. Organomet. Chem.* **2004**, *689*, 2013. (b) Wu, H.-P.; Weakley, T. J. R.; Haley, M. M. *Chem. Eur. J.* **2005**, *11*, 1191.

(10) Iron, M. A.; Martin, J. M. L.; van der Boom, M. E. *J. Am. Chem. Soc.* **2003**, *125*, 13020.

(11) McGinnety, J. A.; Doedens, R. J.; Ibers, J. A. *Inorg. Chem.* **1967**, *6*, 2243.

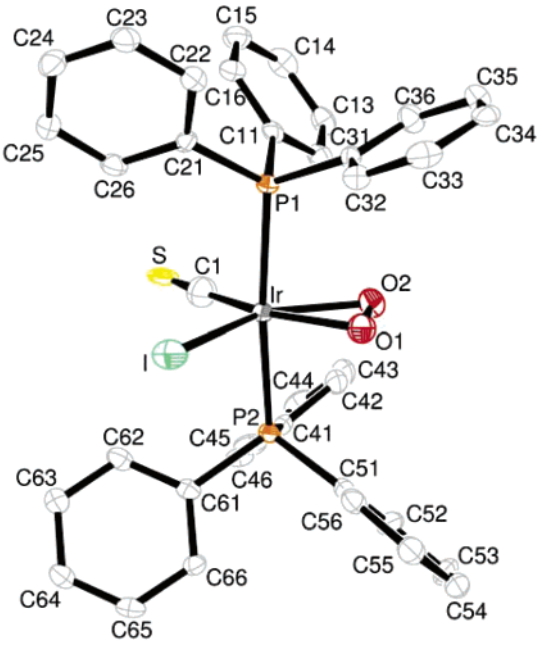

Figure 1. Molecular geometry of $Ir(O_2)I(CS)(PPh_3)_2$ (**2**), showing the atom labeling and atoms as 50% probability displacement ellipsoids.

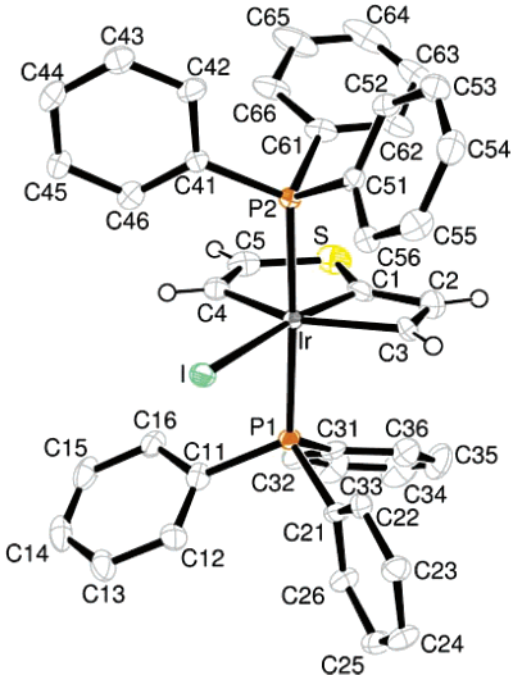

Figure 2. Molecular geometry of $Ir[C_3H_2(CH{=}CHS\text{-}1)]I(PPh_3)_2$ (**3**), showing the atom labeling and atoms as 50% probability displacement ellipsoids.

1.454(8) Å in **2** is shorter than the observed value of 1.509(26) Å in $Ir(O_2)I(CO)(PPh_3)_2$.[11] This would be expected, in view of the reversibility of the dioxygen addition, and could possibly be attributed to the greater π-accepting abilities of the CS ligand. The attachment of the dioxygen is quite symmetrical, with the two Ir−O distances being Ir−O(1) = 2.049(5) Å and Ir−O(2) = 2.035(5) Å. The Ir−I distance is 2.6850(6) Å, which is short compared with the reported values for $Ir(O_2)I(CO)(PPh_3)_2$ (2.767(5) and 2.738(5) Å)[11] and is also shorter than the average for 123 recorded observations for Ir−I bonds in six-coordinate iridium (2.7564 with a SD of 0.060 Å; Cambridge Crystallographic Data Base).

Scheme 4

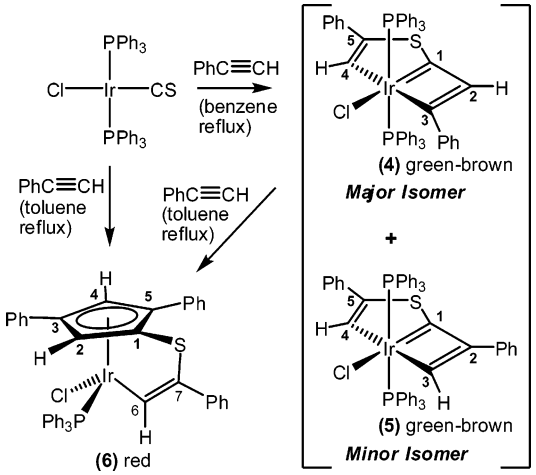

Reaction of $IrI(CS)(PPh_3)_2$ (1) with Ethyne To Form the Tethered Iridacyclobutadiene $Ir[C_3H_2(CH{=}CHS\text{-}1)]I(PPh_3)_2$ (3) and the Crystal Structure of 3. Reaction between $IrI(CS)(PPh_3)_2$ (**1**) and ethyne in benzene at 75 °C leads to the formation of the tethered iridacyclobutadiene $Ir[C_3H_2(CH{=}CHS\text{-}1)]I(PPh_3)_2$ (**3**) as green-brown crystals in reasonable yield (see Scheme 3). Two molecules of ethyne have been incorporated into this product, the first (C2 and C3, see numbering in Scheme 3) combining with the thiocarbonyl ligand to generate a four-membered IrC_3 ring and the second molecule (C4 and C5) effectively alkylating the sulfur atom and in so doing forming a five-membered ring back to the iridium atom. Although excess ethyne was available as a reactant in the preparation of **3**, there was no evidence for any further insertion of ethyne into either the four-membered or five-membered iridacyclic rings. Unambiguous characterization of this substituent-free iridabicyclic complex follows from ^1H and ^{13}C NMR spectra. In the ^1H NMR spectrum the most downfield signal at 12.06 ppm is assigned to H3 and appears as a doublet ($^3J_{HH}$ = 5.1 Hz) coupling to H2, which is assigned to the multiplet signal at 8.35 ppm. The other Ir−C*H*, which is H4, appears as a doublet ($^3J_{HH}$ = 7.9 Hz) at 9.83 ppm, and H5 appears at 6.88 ppm as a doublet of triplets ($^3J_{HH}$ = 7.9 Hz, $^4J_{PH}$ = 1.5 Hz). In the ^{13}C NMR spectrum the most downfield *C*H signal is again associated with C3 in the iridacyclobutadiene ring, which appears as a triplet signal at 177.6 ppm ($^2J_{PC}$ = 9.3 Hz), while C4 appears as a triplet signal at 157.1 ppm ($^2J_{PC}$ = 9.1 Hz). C2 and *C*5 appear at 147.7 and 139.2 ppm, respectively, also as triplet signals. The remaining iridium-bound iridacyclobutadiene carbon, C1, appears as a triplet at 211.8 ppm ($^2J_{PC}$ = 5.1 Hz), the very downfield position reflecting the multiple-bond character in this Ir−C bond. In the ^{31}P NMR spectrum the two equivalent phosphorus atoms appear as a singlet at −10.13 ppm. To confirm the structure of **3** and to gain further information relating to the iridacyclobutadiene ring, an X-ray crystal structure determination of **3** was undertaken.

The molecular structure of **3** is shown in Figure 2, and selected bond distances and angles are collected in Table 3. The geometry about iridium is close to octahedral, with the two triphenylphosphine ligands arranged trans to one another, and the bicyclic ring system is essentially planar. The Ir−C(1) bond is easily the shortest of the three Ir−C bonds at 1.940(8) Å, suggesting a bond order approaching 2. The bond distances Ir−C(3) and Ir−C(4), on the other hand, are appropriate for single bonds at 2.125(8) and 2.070(10) Å, respectively. In keeping with these observed Ir−C single bonds, the measured distances for C(2)−C(3) and C(4)−C(5) are 1.337(14) and 1.331(13) Å,

Table 1. Data Collection and Processing Parameters for Compounds 2−8

	2·CH_2Cl_2	**3**·CH_2Cl_2	**4**·$2CH_2Cl_2$	**5**·CH_2Cl_2·$3C_2H_6O$	**6**·CH_2Cl_2	**7**·$3CDCl_3$	**8**·$1.75C_6H_6$
formula	$C_{37}H_{30}IIrO_2P_2S$·CH_2Cl_2	$C_{41}H_{34}IIrP_2S$·CH_2Cl_2	$C_{53}H_{42}ClIrP_2S$·$2CH_2Cl_2$	$C_{53}H_{42}ClIrP_2S$·CH_2Cl_2·$3C_2H_6O$	$C_{43}H_{33}ClIrPS$·CH_2Cl_2	$C_{45}H_{38}IIrO_4P_2S$·$3CDCl_3$	$C_{49}H_{42}ClIrO_6P_2S$·$1.75C_6H_6$
mol wt	1004.64	1024.71	1170.40	1223.65	1850.60	1417.00	1185.17
cryst syst	monoclinic	monoclinic	monoclinic	triclinic	triclinic	triclinic	monoclinic
space group	$P2_1/n$	$P2_1$	$P2_1$	$P\bar{1}$	$P\bar{1}$	$P\bar{1}$	$P2_1/c$
a, Å	10.6388(2)	12.0872(3)	11.9631(2)	10.6941(1)	9.9230(1)	11.8918(1)	12.0065(4)
b, Å	22.4279(5)	14.3121(3)	11.567292)	12.0101(1)	14.4690(1)	13.5695(1)	19.2784(6)
c, Å	14.9570(3)	12.0945(3)	17.7181(1)	19.9108(1)	14.5649(1)	18.9304(2)	22.4702(8)
α, deg	90.0	90.0	90.0	85.507(1)	91.269(1)	70.741(1)	90.0
β, deg	92.459(1)	114.590(1)	95.758(1)	83.165(1)	108.801(1)	85.553(1)	100.255(1)
γ, deg	90.0	90.0	90.0	80.417(1)	106.762(1)	65.585(1)	90.0
V, Å^3	3565.54(13)	1902.52(8)	2439.45(6)	2499.20(3)	1880.14(2)	2619.74(4)	5118.0(3)
T, K	85(2)	85(2)	83(2)	83(2)	83(2)	84(2)	83(2)
Z	4	2	2	2	2	2	4
d(calcd), g cm^{-3}	1.872	1.789	1.593	1.626	1.634	1.796	1.538
F(000)	1944	996	1168	1240	916	1380	2390
μ, mm^{-1}	4.943	4.630	3.157	2.986	3.894	3.740	2.817
cryst size, mm	0.20 × 0.20 × 0.06	0.42 × 0.34 × 0.30	0.26 × 0.20 × 0.08	0.40 × 0.20 × 0.20	0.38 × 0.22 × 0.12	0.30 × 0.16 × 0.10	0.34 × 0.20 × 0.20
2*θ* (min, max), deg	4.24, 52.82	3.70, 54.30	3.94, 52.70	4.12, 50.04	3.92, 54.22	1.74, 25.70	1.72, 25.68
no. of rflns collected	21 250	12 203	14 814	24 876	19 213	24 044	29 039
no. of indep rflns	7286	7714	9194	8816	8156	9896 (R_{int} = 0.0395)	29 039 (R_{int} = 0.0216)
T (min, max)	0.5171, 0.7719	0.2466, 0.3372	0.71877, 0.84328	0.461 99, 0.660 35	0.3193, 0.6523	0.4000, 0.7061	0.4476, 0.6027
goodness of fit on F^2	1.027	0.986	1.018	1.128	1.041	1.035	1.086
R1, wR2 (obsd data)[a]	0.0451, 0.1162	0.0412, 0.1079	0.0313, 0.0762	0.0772, 0.1894	0.0208, 0.0501	0.0285, 0.0644	0.0246, 0.0534
R1, wR2 (all data)	0.0556, 0.1233	0.0419, 0.1091	0.0324, 0.0771	0.0831, 0.1930	0.0231, 0.0514	0.0348, 0.0666	0.0306, 0.0567

[a] $R1 = \sum||F_o| - |F_c||/\sum|F_o|$; $wR2 = \{\sum[w(F_o^2 - F_c^2)^2]/\sum[w(F_o^2)^2]\}^{1/2}$.

Table 2. Selected Bond Lengths (Å) and Angles (deg) for 2

Bond Lengths			
Ir−C(1)	1.833(9)	Ir−P(1)	2.3782(17)
Ir−O(2)	2.035(5)	Ir−I	2.6850(6)
Ir−O(1)	2.049(5)	O(1)−O(2)	1.454(8)
Ir−P(2)	2.3695(17)		
Bond Angles			
C(1)−Ir−O(2)	117.5(3)	C(1)−Ir−I	105.2(3)
O(2)−Ir−O(1)	41.7(2)	O(1)−Ir−I	95.54(16)
P(2)−Ir−P(1)	171.73(6)		

Table 3. Selected Bond Lengths (Å) and Angles (deg) for 3

Bond Lengths			
Ir−C(1)	1.940(8)	S−C(1)	1.661(9)
Ir−C(4)	2.070(10)	S−C(5)	1.739(11)
Ir−C(3)	2.125(8)	C(3)−C(2)	1.337(14)
Ir−P(1)	2.3487(15)	C(2)−C(1)	1.491(14)
Ir−P(2)	2.3513(15)	C(4)−C(5)	1.331(13)
Ir−I	2.7810(5)		
Bond Angles			
C(1)−Ir−C(4)	84.3(4)	C(2)−C(3)−Ir	97.7(6)
C(3)−Ir−C(1)	63.4(4)	C(3)−C(2)−C(1)	98.3(8)
C(4)−Ir−C(3)	147.7(3)	C(2)−C(1)−S	137.2(7)
C(1)−Ir−I	172.6(3)	C(2)−C(1)−Ir	100.7(6)
C(4)−Ir−I	102.7(3)	S−C(1)−Ir	122.0(5)
C(3)−Ir−I	109.7(3)	C(4)−C(5)−S	122.2(8)
C(1)−S−C(5)	96.7(4)	C(5)−C(4)−Ir	114.7(7)

respectively, values which are indicative of double bonds between these carbon atoms. Furthermore, the measured C(1)−C(2) distance is 1.491(14) Å, indicative of a single bond. Therefore, the valence bond structure used to depict complex **3** in Scheme 3 is quite appropriate: i.e., there is no evidence for any significant bond delocalization in either the iridacyclobutadiene ring or the fused iridathiophene ring. The Ir−I distance is 2.7810(5) Å, longer than the same distance in the dioxygen adduct, complex **2**, which is 2.6850(6) Å, and longer than the average value in the Cambridge Crystallographic Data Base (see above). This reflects the different trans influencr of a "carbene" carbon atom relative to that of a "peroxide" oxygen atom.

Reaction of IrCl(CS)(PPh$_3$)$_2$ with Phenylacetylene To Form the Isomeric Tethered Iridacyclobutadienes Ir[C$_3$H(CH═C{Ph}S-1)(Ph-3)]Cl(PPh$_3$)$_2$ (4) and Ir[C$_3$H(CH═C{Ph}S-1)(Ph-2)]Cl(PPh$_3$)$_2$ (5) and the Crystal Structures of 4 and 5. To explore the direction of addition of a substituted alkyne, reaction between IrCl(CS)(PPh$_3$)$_2$ and phenylacetylene was investigated. As shown in Scheme 4, two green-brown isomers of a product analogous to complex **3** were detected, arising from the direction of addition of the phenylacetylene in the formation of the iridacyclobutadiene ring. Both compounds have the same arrangement of the phenylacetylene in the five-membered ring. The major isomer, Ir[C$_3$H(CH═C{Ph}S-1)(Ph-3)]Cl(PPh$_3$)$_2$ (**4**), has the phenyl substituent in the iridacyclobutadiene ring on the α-carbon atom: i.e., C(3). The minor isomer, Ir[C$_3$H(CH═C{Ph}S-1)(Ph-2)]Cl(PPh$_3$)$_2$ (**5**), has the phenyl substituent in the iridacyclobutadiene ring on the *β*-carbon atom: i.e., C(2). Complex **5** was formed in an impure state and in a yield of less than 5%. It was therefore not possible to collect comprehensive experimental data for this compound; however, a single crystal suitable for X-ray analysis was obtained and the characterization of **5** rests mainly on the structure determination (see below). In the ^{1}H NMR spectrum of **4** the two ring protons H2 and H4 appear at 9.61 and 8.57 ppm, respectively, with H4 showing weak phosphorus coupling ($^3J_{PH}$ = 3.0 Hz). In the ^{13}C NMR spectrum the most downfield carbon signal is again associated with C1 in the iridacyclobutadiene ring, which appears as a triplet signal at 206.3 ppm ($^2J_{PC}$ = 5.4 Hz), while C2 appears as a triplet signal at 141.2 ppm ($^3J_{PC}$ = 4.6 Hz) and C3 as a triplet signal at 195.3 ppm ($^2J_{PC}$ = 8.4 Hz). In the five-membered ring C4 is observed as a triplet signal at 151.8 ppm ($^2J_{PC}$ = 10.7 Hz) and C5 as a singlet at 139.1 ppm. In the ^{31}P

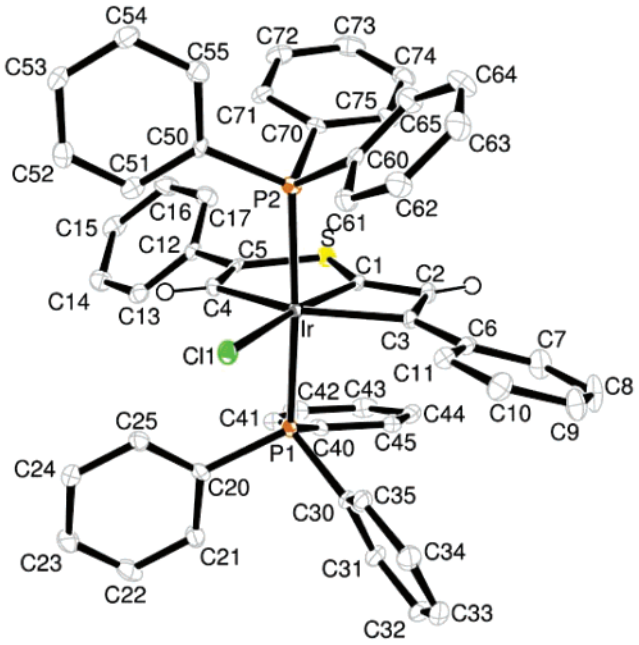

Figure 3. Molecular geometry of Ir[C_3H(CH═C{Ph}S-1)(Ph-3)]-Cl(PPh_3)$_2$ (**4**), showing the atom labeling and atoms as 50% probability displacement ellipsoids.

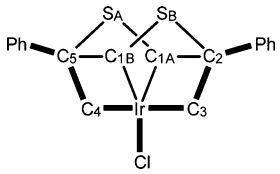

Figure 4. Diagram illustrating the disorder of C1 and S atoms in the crystal structure of complex **5**.

Table 4. Selected Bond Lengths (Å) and Angles (deg) for 4

Bond Lengths			
Ir−C(1)	1.940(5)	S−C(5)	1.798(7)
Ir−C(4)	2.097(6)	C(1)−C(2)	1.420(9)
Ir−C(3)	2.125(6)	C(2)−C(3)	1.389(9)
Ir−P(1)	2.3541(10)	C(3)−C(6)	1.473(8)
Ir−P(2)	2.3615(13)	C(4)−C(5)	1.338(9)
Ir−Cl(1)	2.4953(12)	C(5)−C(12)	1.496(8)
S−C(1)	1.685(6)		
Bond Angles			
P(1)−Ir−P(2)	176.10(11)	S−C(1)−Ir	122.4(3)
C(4)−Ir−Cl(1)	105.39(18)	C(3)−C(2)−C(1)	100.4(5)
C(3)−Ir−Cl(1)	106.40(18)	C(2)−C(3)−Ir	94.2(4)
C(1)−S−C(5)	97.1(3)	C(5)−C(4)−Ir	116.7(5)
C(2)−C(1)−Ir	101.5(4)	C(4)−C(5)−S	119.5(5)

NMR spectrum the two equivalent phosphorus atoms appear as a singlet at −12.48 ppm. The ^{1}H NMR spectroscopic data collected for **5** are restricted to a signal at 12.78 ppm for H3 and a signal at 10.03 ppm for H4. In the ^{31}P NMR spectrum of **5** the two equivalent phosphorus atoms appear as a singlet at −4.38 ppm. To confirm the structures of **4** and **5**, X-ray crystal structure determinations were undertaken.

The molecular structure of **4** is shown in Figure 3, and selected bond distances and angles are collected in Table 4. The geometry about iridium is closely related to that observed for complex **3** described above. The Ir−C(1) bond distance of 1.940(5) Å is identical with that found for **3** and again is much shorter than the other two Ir−C bonds. The bond distances Ir−C(3) = 2.125(6) Å and Ir−C(4) = 2.097(6) Å are very close to those for complex **3** and are again indicative of these being

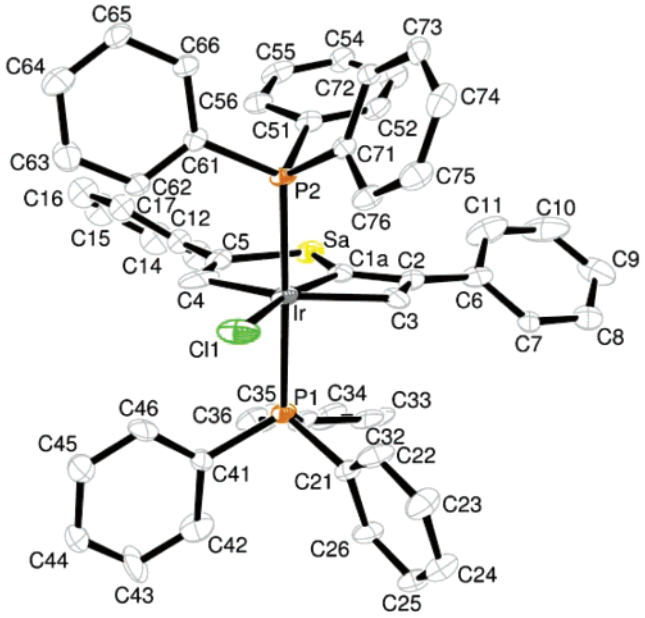

Figure 5. Molecular geometry of Ir[C_3H(CH═C{Ph}S-1)(Ph-2)]-Cl(PPh_3)$_2$ (**5**), showing the atom labeling and atoms as 50% probability displacement ellipsoids. Only the major component of the disorder model (see Figure 4) is shown.

Table 5. Selected Bond Lengths (Å) and Angles (deg) for 5

Bond Lengths			
Ir−C(1B)	1.915(19)	SB−C(1B)	1.67(2)
Ir−C(1A)	1.953(15)	SB−C(2)	1.947(16)
Ir−C(4)	2.054(14)	C(1A)−C(2)	1.44(2)
Ir−C(3)	2.107(12)	C(1B)−C(5)	1.40(2)
Ir−P(2)	2.331(2)	C(2)−C(3)	1.374(18)
Ir−P(1)	2.332(2)	C(2)−C(6)	1.454(17)
Ir−Cl(1)	2.481(3)	C(4)−C(5)	1.36(2)
SA−C(1A)	1.60(2)	C(5)−C(12)	1.461(16)
SA−C(5)	1.915(15)		
Bond Angles			
C(1A)−Ir−C(4)	89.0(7)	SA−C(1A)−Ir	124.0(10)
C(1B)−Ir−C(3)	95.2(7)	SB−C(1B)−Ir	120.6(12)
P(2)−Ir−P(1)	177.74(9)	C(3)−C(2)−C(1A)	92.3(11)
C(1A)−SA−C(5)	93.1(7)	C(2)−C(3)−Ir	101.5(10)
C(1B)−SB−C(2)	92.4(8)	C(5)−C(4)−Ir	109.4(11)
C(2)−C(1A)−SA	129.6(12)	C(4)−C(5)−C(1B)	81.5(12)
C(2)−C(1A)−Ir	106.4(12)		

single bonds. The observed distances for C(2)−C(3) and C(4)−C(5) are 1.389(9) and 1.338(9) Å, respectively, values which are appropriate for a somewhat delocalized bond between C(2)−C(3) and for a double bond between C(4)−C(5). The C(1)−C(2) distance is 1.420(9) Å. The Ir−Cl distance is 2.4953(12) Å, which is long when compared with the average for 572 recorded observations for Ir−Cl bonds in six-coordinate iridium (2.4046 Å with a SD of 0.066 Å; Cambridge Crystallographic Data Base). This reflects the strong trans influence of the "carbene" carbon atom (C1) in the iridacyclobutadiene ring. The elongating effect of a genuine carbene ligand on the Ir−Cl bond is well-illustrated in the structure of $IrCl_3$(═CCl_2)(PPh_3)$_2$, where Ir−Cl (trans to CCl_2) is 2.407(2) Å, whereas Ir−Cl (trans to Cl) is 2.359(1) Å.[12]

The crystal structure of **5** is disordered, and a diagram illustrating the disorder of C1 and S atoms in the crystal structure is shown in Figure 4. The molecular geometry of the major component of the disorder model is shown in Figure 5. Selected bond distances and angles are collected in Table 5. The Ir−

(12) Clark, G. R.; Roper, W. R.; Wright, A. H. *J. Organomet. Chem.* **1982**, *236*, C7.

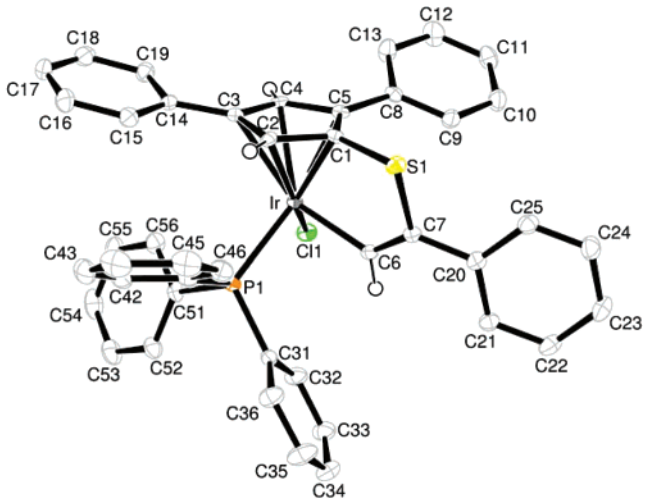

Figure 6. Molecular geometry of Ir[η^5-C_5H_2(SCPh=CH-1)(Ph-3)(Ph-5)]Cl(PPh_3) (**6**), showing the atom labeling and atoms as 50% probability displacement ellipsoids.

Table 6. Selected Bond Lengths (Å) and Angles (deg) for 6

	Bond Lengths		
Ir−C(6)	2.029(2)	C(1)−C(2)	1.443(3)
Ir−C(1)	2.122(2)	C(1)−C(5)	1.467(3)
Ir−C(2)	2.175(2)	C(2)−C(3)	1.449(3)
Ir−C(5)	2.245(2)	C(3)−C(4)	1.418(4)
Ir−P(1)	2.2858(6)	C(3)−C(14)	1.478(4)
Ir−C(4)	2.320(2)	C(4)−C(5)	1.451(4)
Ir−C(3)	2.370(2)	C(5)−C(8)	1.479(3)
Ir−Cl(1)	2.3818(6)	C(6)−C(7)	1.354(3)
S(1)−C(1)	1.773(3)	C(7)−C(20)	1.481(3)
S(1)−C(7)	1.798(2)		
	Bond Angles		
P(1)−Ir−Cl(1)	89.93(2)	C(4)−C(3)−C(2)	106.5(2)
C(1)−S(1)−C(7)	97.55(11)	C(3)−C(4)−C(5)	111.2(2)
C(2)−C(1)−C(5)	108.3(2)	C(4)−C(5)−C(1)	105.1(2)
C(2)−C(1)−S(1)	122.48(18)	C(7)−C(6)−Ir	121.46(18)
C(5)−C(1)−S(1)	128.98(19)	C(6)−C(7)−S(1)	118.51(19)
C(1)−C(2)−C(3)	108.6(2)		

C(1A) bond distance is 1.953(15) Å, similar to that found for **4**. The bond distances Ir−C(3) = 2.107(12) Å and Ir−C(4) = 2.054(14) Å are close to those for complex **4** and are again indicative of these being single bonds. The observed distances for C(2)−C(3) and C(4)−C(5) are 1.374(18) and 1.36(2) Å, respectively, values which are appropriate for a somewhat delocalized bond between C(2) and C(3) and for a double bond between C(4) and C(5). The C(1A)−C(2) distance is 1.44(2) Å. The Ir−Cl distance is 2.481(3) Å, which is longer than the average for 572 recorded observations for Ir−Cl bonds in six-coordinate iridium (2.4046 Å with a SD of 0.066 Å; Cambridge Crystallographic Data Base), clearly reflecting the marked trans influence of C(1), which is effectively a carbene carbon. Similar observations have already been made for complex **4**.

Thermal Reaction of Ir[C_3H(CH=C{Ph}S-1)(Ph-3)]Cl(PPh_3)$_2$ (4) with Phenylacetylene To Form the Tethered Cyclopentadienyl Complex Ir[η^5-C_5H_2(SCPh=CH-1)(Ph-3)(Ph-5)]Cl(PPh_3) (6) and the Crystal Structure of 6. Of the three tethered iridacyclobutadiene complexes described in this paper, **3**, **4**, and **7** (see below), only complex **4** reacted with an excess of the added acetylene at an elevated temperature to give as the ultimate product a tethered cyclopentadienyl complex. As shown in Scheme 4, when complex **4** is heated with excess phenylacetylene at toluene reflux, the red, tethered cyclopentadienyl complex Ir[η^5-C_5H_2(SCPh=CH-1)(Ph-3)(Ph-5)]Cl(PPh_3) (**6**) is formed in high yield. The same compound is formed when IrCl(CS)(PPh_3)$_2$ is heated with excess phenylacetylene in toluene at reflux, but the yield is lower. A feature unique to complex **4**, which may contribute to this particular reactivity, is the presence of a substituent (phenyl) on the α-carbon atom of the iridacyclobutadiene ring. It is probable that this reaction proceeds through an intermediate tethered iridabenzene complex (formed through insertion of the acetylene into the iridacyclobutadiene ring) and subsequent elimination of the C_5 fragment as a cyclopentadienyl ligand (see Introduction, Scheme 2).[10] In the ^{1}H NMR spectrum of **6** the two Cp ring protons H2 and H4 appear as doublets at 5.11 ($^4J_{HH}$ = 2.0 Hz) and 6.93 ($^4J_{HH}$ = 2.0 Hz) ppm. The iridium-bound C*H* of the tethering arm (H6) appears as a doublet at 8.09 ppm ($^3J_{PH}$ = 7.5 Hz). In the ^{13}C NMR spectrum the most downfield carbon signal is C7, which appears as a doublet at 163.3 ppm ($^3J_{PC}$ = 4.0 Hz), while C6 appears at 130.4 ppm. The cyclopentadienyl ring carbons are observed at 82.5 (C2 or C4), 85.8 (C1), 93.2 (C3 or C5), 100.6 (C3 or C5), and 102.1 (C2 or C4) ppm. C1 alone shows phosphorus coupling ($^2J_{PC}$ = 15.1 Hz), and the structural data to be discussed below show that Ir−C(1) is considerably shorter than the other Ir−C(2−5) distances: i.e., the tethered Cp ring is displaced away from a symmetrical bonding position. In the ^{31}P NMR spectrum the single phosphorus atom appears at 1.63 ppm.

Scheme 5

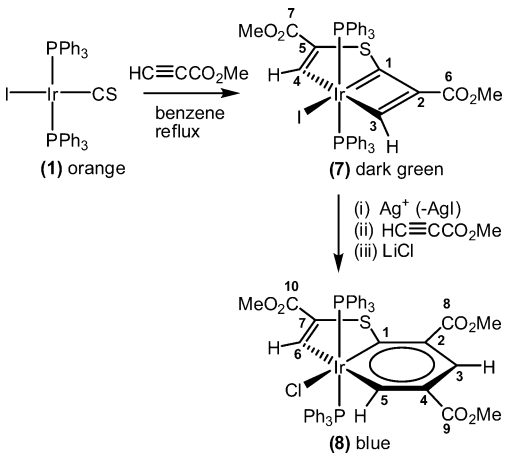

The molecular structure of **6** is shown in Figure 6, and selected bond distances and angles are collected in Table 6. As is the case for other $CpML_3$ complexes, the geometry about iridium in **6** is that of a piano stool, with the presence of the tether causing a displacement of the Cp ligand. This is clearly revealed by the Ir−C distances, which are as follows (Å): Ir−C(1) = 2.122(2), Ir−C(2) = 2.175(2), Ir−C(3) = 2.370(2), Ir−C(4) = 2.320(2), Ir−C(5) = 2.245(2) Å. The Ir−C(6) distance is 2.029(2) Å, and the C(6)−C(7) distance is 1.354(3) Å. The Ir−Cl distance is 2.3818(6) Å, which in this very different geometrical environment is much shorter than the values found in complexes **4** and **5** but is comparable to the values found (2.408(3) and 2.406(3) Å) in the structurally related cyclopentadienyl complex Cp*$IrCl_2$(PPh_3).[13]

Reaction of IrI(CS)(PPh_3)$_2$ (1) with Methyl Propiolate To Form the Tethered Iridacyclobutadiene Ir[C_3H(CH=C{CO_2Me}S-1)(CO_2Me-2)]I(PPh_3)$_2$ (7) and the Crystal Structure of 7. As shown in Scheme 5, when IrI(CS)(PPh_3)$_2$ (**1**) is

(13) Le Bras, J.; Amouri, H.; Vaissermann, J. *J. Organomet. Chem.* **1997**, *548,* 305.

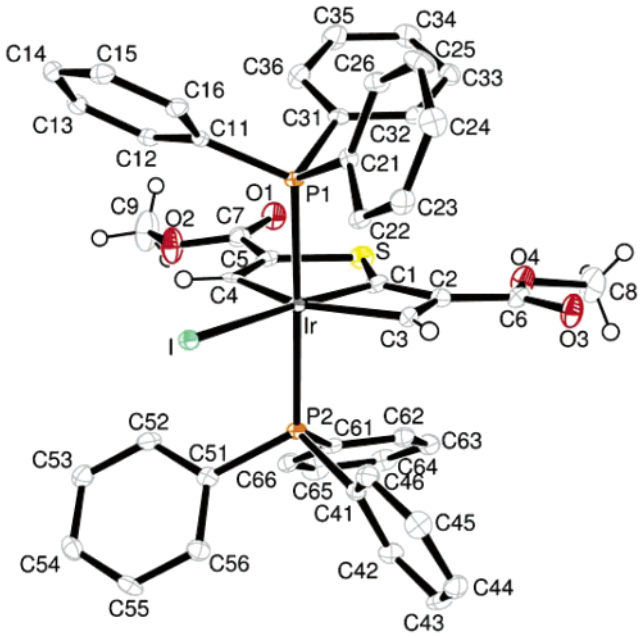

Figure 7. Molecular geometry of Ir[C_3H(CH═C{CO_2Me}S-1)(CO_2Me-2)]I(PPh_3)$_2$ (**7**), showing the atom labeling and atoms as 50% probability displacement ellipsoids.

heated at benzene reflux with an excess of methyl propiolate, the dark green tethered iridacyclobutadiene Ir[C_3H(CH═C{CO_2Me}S-1)(CO_2Me-2)]I(PPh_3)$_2$ (**7**) is formed. It can be noted that this compound has the same positioning of substituents on the four- and five-membered rings as was found in complex **5**. No evidence was found for the formation of any other isomers, as was the case in the reactions with phenylacetylene (see above). Treatment of **1** with excess methyl propiolate at elevated temperatures gave no indication of the formation of a tethered Cp complex analogous to complex **6**. In the ^{1}H NMR spectrum of **7** the two ring protons H3 and H4 appear at 13.23 and 11.45 ppm, respectively, both signals appearing as singlets. In the ^{13}C NMR spectrum the most downfield carbon signal is again associated with C1 in the iridacyclobutadiene ring, which appears as a triplet signal at 214.2 ppm ($^2J_{PC}$ = 4.4 Hz), while C2 appears as a triplet signal at 153.5 ppm ($^3J_{PC}$ = 4.5 Hz) and C3 as a triplet signal at 198.9 ppm ($^2J_{PC}$ = 10.6 Hz). These values are all close to those discussed above for complexes **3** and **4**. In the five-membered ring C4 is observed as a triplet signal at 177.9 ppm ($^2J_{PC}$ = 8.5 Hz) and C5 as a singlet at 148.8 ppm. In the ^{31}P NMR spectrum the two equivalent phosphorus atoms appear as a singlet at −8.75 ppm.

A crystal structure determination of complex **7** revealed the same basic geometry for the tethered iridacyclobutadiene skeleton that had been found in complexes **3**−**5**. The molecular geometry of **7** is shown in Figure 7. Selected bond distances and angles are collected in Table 7. The Ir−C(1) bond distance of 1.941(4) Å is similar to those found for **3**−**5**. The bond distances Ir−C(3) = 2.137(4) Å and Ir−C(4) = 2.042(3) Å are close to those for complexes **3**−**5** and are again indicative of these being single bonds. The observed distances for C(2)−C(3) and C(4)−C(5) are 1.373(6) and 1.342(5) Å, respectively, values which are appropriate for a somewhat delocalized bond between C(2) and C(3) and for a double bond between C(4) and C(5). The C(1)−C(2) distance is 1.440(5) Å. The Ir−I distance of 2.7763(3) Å is very close to that found in complex **3** (2.7810(5) Å) and is long compared with the average for 123 recorded observations for Ir−I bonds in six-coordinate iridium (2.7564 Å with a SD of 0.060 Å; Cambridge Crystallographic Data Base).

Table 7. Selected Bond Lengths (Å) and Angles (deg) for 7

Bond Lengths			
Ir−C(1)	1.941(4)	S−C(5)	1.806(4)
Ir−C(4)	2.042(3)	C(1)−C(2)	1.440(5)
Ir−C(3)	2.137(4)	C(2)−C(3)	1.373(6)
Ir−P(1)	2.3594(9)	C(2)−C(6)	1.471(5)
Ir−P(2)	2.3696(9)	C(4)−C(5)	1.342(5)
Ir−I	2.7763(3)	C(5)−C(7)	1.476(5)
S−C(1)	1.670(4)		
Bond Angles			
C(1)−Ir−C(4)	84.66(15)	P(2)−Ir−I	87.04(2)
C(1)−Ir−C(3)	63.46(15)	C(1)−S−C(5)	95.23(18)
C(4)−Ir−C(3)	148.10(15)	C(2)−C(1)−S	135.0(3)
C(1)−Ir−P(1)	92.77(11)	C(2)−C(1)−Ir	101.7(2)
C(4)−Ir−P(1)	91.71(10)	S−C(1)−Ir	123.2(2)
C(3)−Ir−P(1)	89.15(10)	C(3)−C(2)−C(1)	99.7(3)
C(1)−Ir−P(2)	92.84(11)	C(3)−C(2)−C(6)	129.8(3)
C(4)−Ir−P(2)	93.31(10)	C(1)−C(2)−C(6)	130.4(3)
C(3)−Ir−P(2)	89.31(10)	C(2)−C(3)−Ir	95.1(2)
P(1)−Ir−P(2)	172.79(3)	C(5)−C(4)−Ir	116.6(3)
C(1)−Ir−I	172.80(10)	C(4)−C(5)−C(7)	129.5(4)
C(4)−Ir−I	102.54(11)	C(4)−C(5)−S	120.3(3)
C(3)−Ir−I	109.35(10)	C(7)−C(5)−S	110.2(3)
P(1)−Ir−I	86.83(2)		

Ring Expansion of the Tethered Iridacyclobutadiene Ir[C_3H(CH═C{CO_2Me}S-1)(CO_2Me-2)]I(PPh_3)$_2$ (7) through Sequential Treatment First with AgO_3SCF_3, Followed by Methyl Propiolate and LiCl, To Form the Tethered Iridabenzene Ir[C_5H_2(CH═C{CO_2Me}S-1)(CO_2Me-2)(CO_2Me-4)]Cl(PPh_3)$_2$ (8) and the Crystal Structure of 8. Under the conditions used for the preparation of complex **7**, there was no indication of further reaction with the excess methyl propiolate present. This could be attributed to the inertness of the octahedral iridium(III) complex toward ligand dissociation, which in turn prevents further methyl propiolate coordinating to iridium as a prelude to expansion of the four-membered ring. We therefore explored the use of silver triflate as a reagent to remove the iodide ligand as silver iodide from complex **7**, thus facilitating coordination of methyl propiolate, which was added in a subsequent step. As depicted in Scheme 5, this strategy is successful and addition of lithium chloride to the blue-green solution resulting from sequential addition of silver triflate and methyl propiolate to **7** at room temperature allowed isolation of the blue tethered iridabenzene Ir[C_5H_2(CH═C{CO_2Me}S-1)(CO_2Me-2)(CO_2Me-4)]Cl(PPh_3)$_2$ (**8**) in high yield. It can be noted here that similar ring-expansion reactions, using silver triflate followed by methyl propiolate, were attempted with both complexes **3** and **4** but led only to intractable mixtures. This successful synthesis of **8** represents a verification of the often postulated ring-expansion step converting a metallacyclobutadiene to a metallabenzene through reaction with an acetylene.[8,9] A possibly related observation is the ultimate formation of a cyclopentadienyl complex (from two acetylene moieties and a CS ligand) via a postulated metallabenzene intermediate, which in turn may arise from a related ring-expansion reaction.[14]

In the ^{1}H NMR spectrum of **8** the two protons in the six-membered iridabenzene ring, H3 and H5, appear as doublets at 7.63 ($^4J_{HH}$ = 2.4 Hz) and 13.25 ($^4J_{HH}$ = 2.4 Hz) ppm, respectively. These chemical shifts are entirely consistent with those of other reported iridabenzenes.[12] H6, in the five-membered tethering ring, appears as a singlet at 10.70 ppm. In

(14) Hill, A. F.; Schultz, M.; Willis, A. C. *Organometallics* **2005**, *24*, 2027.

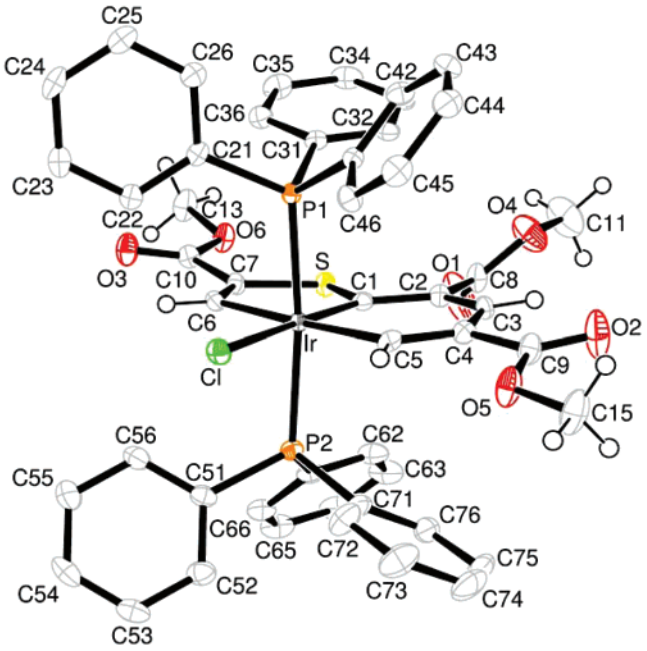

Figure 8. Molecular geometry of Ir[C_5H_2(CH═C{CO_2Me}S-1)(CO_2Me-2)(CO_2Me-4)]Cl(PPh_3)$_2$ (**8**), showing the atom labeling and atoms as 50% probability displacement ellipsoids.

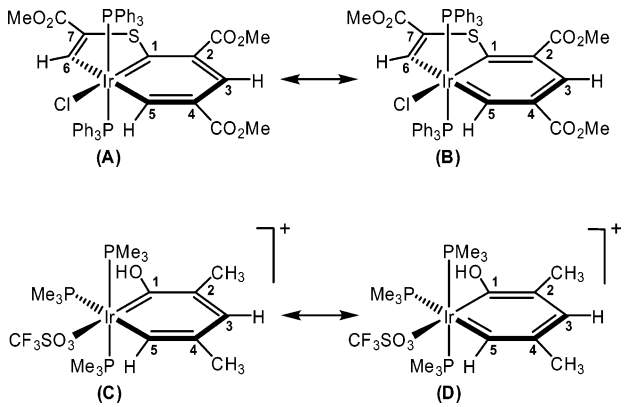

Figure 9. Contributing valence bond structures for complex **8** and for the related iridaphenol.

the ^{13}C NMR spectrum the iridium-bound carbon atoms C1 and C5 appear as triplets at characteristic downfield positions of 252.7 ($^2J_{PC}$ = 2.8 Hz) and 247.5 ($^2J_{PC}$ = 7.8 Hz) ppm. These positions are conspicuously further downfield than the positions observed in any of the tethered iridacyclobutadiene complexes **3**, **4**, and **7** and are consistent with significant multiple bonding in both the Ir−C(1) and Ir−C(5) bonds. The remaining three iridabenzene ring carbon atoms all appear as singlets at 124.0 (C2), 162.0 (C3), and 126.8 (C4) ppm. In the five-membered ring C6 is observed as a triplet signal at 198.2 ppm ($^2J_{PC}$ = 11.0 Hz) and C7 also as a triplet at 143.7 ppm ($^3J_{PC}$ = 2.5 Hz). In the ^{31}P NMR spectrum the two equivalent phosphorus atoms appear as a singlet at −0.34 ppm.

A crystal structure determination of complex **8** confirmed the presence of the tethered iridabenzene and provided structural evidence for delocalization of bonds within the six-membered ring. The molecular geometry of **8** is shown in Figure 8. Selected bond distances and angles are collected in Table 8. In comparison with all of the tethered iridacyclobutadiene complexes, the two Ir−C bonds in the six-membered ring tend toward equalization, with Ir−C(1) being 1.973(3) Å and Ir−C(5) being 2.042(3) Å, values intermediate between single and

Table 8. Selected Bond Lengths (Å) and Angles (deg) for 8

Bond Lengths			
Ir−C(1)	1.973(3)	C(1)−C(2)	1.449(4)
Ir−C(5)	2.042(3)	C(2)−C(3)	1.361(4)
Ir−C(6)	2.106(3)	C(2)−C(8)	1.515(4)
Ir−P(1)	2.3622(7)	C(3)−C(4)	1.434(4)
Ir−P(2)	2.3667(8)	C(4)−C(5)	1.360(4)
Ir−Cl	2.4685(7)	C(4)−C(9)	1.480(4)
S−C(1)	1.722(3)	C(6)−C(7)	1.341(4)
S−C(7)	1.765(3)	C(7)−C(10)	1.477(4)
Bond Angles			
C(1)−Ir−C(5)	91.39(12)	C(2)−C(1)−S	114.6(2)
C(1)−Ir−C(6)	84.17(12)	C(2)−C(1)−Ir	125.5(2)
C(5)−Ir−C(6)	175.49(11)	S−C(1)−Ir	119.84(16)
C(1)−Ir−P(1)	91.11(8)	C(3)−C(2)−C(1)	124.5(3)
C(5)−Ir−P(1)	93.10(8)	C(3)−C(2)−C(8)	116.0(3)
C(6)−Ir−P(1)	86.17(8)	C(1)−C(2)−C(8)	119.5(3)
C(1)−Ir−P(2)	94.93(8)	C(2)−C(3)−C(4)	128.2(3)
C(5)−Ir−P(2)	89.53(8)	C(5)−C(4)−C(3)	121.8(3)
C(6)−Ir−P(2)	91.67(8)	C(5)−C(4)−C(9)	122.6(3)
P(1)−Ir−P(2)	173.35(3)	C(3)−C(4)−C(9)	115.6(3)
C(1)−Ir−Cl	176.46(9)	C(4)−C(5)−Ir	128.3(2)
C(5)−Ir−Cl	85.07(9)	C(7)−C(6)−Ir	117.8(2)
C(6)−Ir−Cl	99.36(8)	C(6)−C(7)−C(10)	124.2(3)
P(1)−Ir−Cl	88.86(2)	C(6)−C(7)−S	119.1(2)
P(2)−Ir−Cl	85.28(2)	C(10)−C(7)−S	116.2(2)
C(1)−S−C(7)	98.80(14)		

double bonds. The carbon−carbon distances within this six-membered ring are as follows (Å): C(1)−C(2) = 1.449(4), C(2)−C(3) = 1.361(4), C(3)−C(4) = 1.434(4), C(4)−C(5) = 1.360(4) Å. These values lie between single- and double-bond distances and are similar to measured carbon−carbon distances in other iridabenzenes,[15] but the delocalization is clearly not perfect and the values suggest that valence bond structure **A** in Figure 9 is more important than **B**. In fact, a very similar set of carbon−carbon distances has been reported for a related "iridaphenol" complex,[16] which is represented in Figure 9 by valence bond structures **C** and **D**. The six-membered iridabenzene ring exhibits a high degree of planarity, the deviations from the mean plane through Ir, C(1), C(2), C(3), C(4), and C(5) being Ir (0.042 Å), C(1) (0.025 Å), C(2) (0.017 Å), C(3) (0.041 Å), C(4) (0.001 Å), and C(5) (0.042 Å). In the five-membered ring the Ir−C(6) distance is 2.106(3) Å, indicative of a single bond, and the C(6)−C(7) distance is 1.341(4) Å, entirely appropriate for a double bond. Clearly there is no structural support for any significant delocalization within the five-membered ring. The Ir−Cl distance of 2.4685(7) Å is shorter than that found in either complex **4** (2.4953(12) Å) or complex **5** (2.481(3) Å) but is still long compared with the average for 572 recorded observations for Ir−Cl bonds in six-coordinate iridium (2.4046 Å with a SD of 0.066 Å; Cambridge Crystallographic Data Base).

Despite the fact that complex **4** reacts with further phenylacetylene under forcing conditions to give as the ultimate product the tethered Cp complex **6** (presumably through the intermediate iridabenzene Ir[C_5H_2(CH═CPhS-1)(Ph-3)(Ph-5)]Cl(PPh_3)$_2$), the ester-substituted iridabenzene Ir[C_5H_2(CH═C{CO_2Me}S-1)(CO_2Me-2)(CO_2Me-4)]Cl(PPh_3)$_2$ is recovered unchanged after heating under reflux in toluene for 1 h. This increased thermal stability, and resistance to elimination of the C_5 fragment as a cyclopentadienyl ligand, may be due to the fact that C(5) is unsubstituted, as well as to the electron-withdrawing nature of the ester substituents and the ring positions of these substituents.

(15) (a) Bleeke, J. R. *Chem. Rev.* **2001**, *101*, 1205. (b) Landorf, C. W.; Haley, M. M. *Angew. Chem., Int. Ed.* **2006**, *45*, 3914.
(16) Bleeke, J. R.; Behm, R. *J. Am. Chem. Soc.* **1997**, *119*, 8503.

A final observation regarding the tethering arm in complex **8**, and also in the tethered iridabutadiene complexes **3**−**5** and **7**, may be appropriate. Because the tethering arm in complex **8** is unsaturated, an alternative way of viewing this molecule would be as a complex which arises from a fusion of an iridabenzene and an iridathiophene: i.e., as an iridabenzothiophene. Likewise the complexes **3**−**5** and **7** could be viewed as arising from a fusion of iridabutadienes and iridathiophenes. We have chosen not to emphasize this point of view mainly because, as discussed above, there is very little evidence for delocalization within the five-membered rings.

Conclusions

The first step in the often postulated ring-expansion reaction of a metallacyclobutadiene with an acetylene, to give first an unstable intermediate metallabenzene and subsequently a stable cyclopentadienyl complex, has been verified by converting a structurally characterized iridacyclobutadiene, Ir[C_3H(CH═C{CO_2-Me}S-1)(CO_2Me-2)]I(PPh_3)$_2$ (**7**), through reaction with methyl propiolate, to a stable iridabenzene, Ir[C_5H_2(CH═C{CO_2Me}S-1)(CO_2Me-2)(CO_2Me-4)]Cl(PPh_3)$_2$ (**8**). This iridabenzene proves to be resistant to conversion to a cyclopentadienyl complex, even under very forcing conditions. However, treatment of another iridacyclobutadiene, Ir[C_3H(CH═C{Ph}S-1)(Ph-3)]Cl-(PPh_3)$_2$ (**4**), involving different ring substituents, with phenylacetylene does not give an isolable iridabenzene but instead forms the tethered cyclopentadienyl complex Ir[η^5-C_5H_2(SCPh═CH-1)(Ph-3)(Ph-5)]Cl(PPh_3) (**6**) directly. The formation of the iridabenzene **8** demonstrates that thiocarbonyl ligands are useful for preparing metallabenzene complexes not only on osmium but also on iridium.

Spectroscopic data are supportive of extensively delocalized bonding in the stable iridabenzene Ir[C_5H_2(CH═C{CO_2Me}S-1)(CO_2Me-2)(CO_2Me-4)]Cl(PPh_3)$_2$ (**8**), but the structural data, while confirming the aromatic nature of the IrC_5 ring, indicates that there is perhaps some localization of the bonds in a pattern which is very similar to that of a previously reported iridaphenol.

Experimental Section

General Procedures and Instruments. Standard laboratory procedures were followed as have been described previously.[17] The compound IrCl(CS)(PPh_3)$_2$[18,19] was prepared according to the literature methods.

Infrared spectra (4000−400 cm^{-1}) were recorded as Nujol mulls between KBr plates on a Perkin-Elmer Paragon 1000 spectrometer. NMR spectra were obtained on either a Bruker DRX 400 or a Bruker Avance 300 instrument at 25 °C. For the Bruker DRX 400, ^{1}H, ^{13}C, and ^{31}P NMR spectra were obtained operating at 400.1 (^{1}H), 100.6 (^{13}C), and 162.0 (^{31}P) MHz, respectively. For the Bruker Avance 300, ^{1}H, ^{13}C, and ^{31}P NMR spectra were obtained operating at 300.13 (^{1}H), 75.48 (^{13}C), and 121.50 (^{31}P) MHz, respectively. Resonances are quoted in ppm and ^{1}H NMR spectra referenced to either tetramethylsilane (0.00 ppm) or the protio impurity in the solvent (7.25 ppm for $CHCl_3$). ^{13}C NMR spectra were referenced to $CDCl_3$ (77.00 ppm) and ^{31}P NMR spectra to 85% orthophosphoric acid (0.00 ppm) as an external standard. Elemental analyses were obtained from the Microanalytical Laboratory, University of Otago.

Preparation of IrI(CS)(PPh_3) (1). Potassium iodide (0.622 g, 3.75 mmol) dissolved in a mixture of ethanol (10 mL) and water (1 mL) was added to a solution of IrCl(CS)(PPh_3)$_2$ (0.600 g, 0.75 mmol) in chloroform (60 mL) under nitrogen. The resulting solution was stirred under nitrogen at room temperature for 18 h, during which time the color became a darker orange. Removal of all the volatiles under vacuum produced a solid which was washed with water, ethanol, and finally hexane. This solid was recrystallized with exclusion of air from dichloromethane/ethanol to give pure **1** as orange needles (0.635 g, 92%). Anal. Calcd for $C_{37}H_{30}IIrP_2S$: C, 50.05; H, 3.40; P, 6.97. Found: C, 49.86; H, 3.58; P, 7.13. IR (cm^{-1}): 1322 s ν(CS). ^{1}H NMR ($CDCl_3$, δ): 7.37−7.80 (m, 30H, P*Ph*$_3$). ^{13}C NMR ($CDCl_3$, δ): 127.8 (broad, P coupling not resolved, *o*-P*Ph*$_3$), 130.1 (s, *p*-P*Ph*$_3$), 135.3 (broad, P coupling not resolved, *m*-P*Ph*$_3$), 240.8 (broad, P coupling not resolved, CS). ^{31}P NMR ($CDCl_3$, δ): 24.36 (s).

Preparation of Ir(O_2)I(CS)(PPh_3) (2). A solution of IrI(CS)-(PPh_3) (**1**; 0.600 g) in CH_2Cl_2 (60 mL) was stirred in air for 1 h, during which time the color changed from orange to a dark red-brown. Addition of ethanol (10 mL) and removal of the CH_2Cl_2 using a rotary evaporator produced pure **2** as a brown microcrystalline solid in quantitative yield. Brown crystals suitable for X-ray study were grown by slow evaporation from a solution in CH_2Cl_2/heptane at room temperature over several days. A crystal structure determination confirmed the presence of one molecule of CH_2Cl_2 of solvation. Anal. Calcd for $C_{37}H_{30}IIrO_2P_2S\cdot CH_2Cl_2$: C, 45.43; H, 3.21. Found: C, 44.80; H, 3.30. IR (cm^{-1}): 1321 s ν(CS); 858 m ν(Ir−O_2). ^{1}H NMR ($CDCl_3$, δ): 7.35−7.62 (m, 30H, P*Ph*$_3$). ^{13}C NMR ($CDCl_3$, δ): 127.6 (t′,[17] $^{1,3}J_{PC}$ = 58.4 Hz, *i*-P*Ph*$_3$), 128.0 (t′, $^{2,4}J_{PC}$ = 10.0 Hz, *o*-P*Ph*$_3$), 130.9 (s, *p*-P*Ph*$_3$), 135.1 (t′, $^{3,5}J_{PC}$ = 10.0 Hz, *m*-P*Ph*$_3$), 259.6 (t, $^2J_{PC}$ = 9.1 Hz, CS). ^{31}P NMR ($CDCl_3$, δ): 5.19 (s).

Preparation of Ir[C_3H_2(CH═CHS-1)I(PPh_3)$_2$ (3). This synthesis may be carried out using either IrI(CS)(PPh_3)$_2$ or IrI(O_2)-(CS)(PPh_3)$_2$ as the starting material. A solution of IrI(O_2)(CS)-(PPh_3)$_2$ (0.310 g, 0.34 mmol) in benzene (30 mL) was placed in a Fisher−Porter bottle and subjected to ethyne under a pressure of 20 psi (*Caution!* A safety shield is needed—potential explosion risk.) with heating at a temperature of 75 °C for 21 h to give a green-brown solution. After the mixture was cooled and the bottle vented, the solvent was removed under reduced pressure to give a brown solid, which was recrystallized from CH_2Cl_2 and EtOH to give pure **3** as a green-brown crystalline solid (0.184 g, 56%). Crystal structure determination confirmed the presence of one molecule of CH_2Cl_2 of solvation. Anal. Calcd for $C_{41}H_{34}IIrP_2S\cdot CH_2Cl_2$: C, 49.23; H, 3.54. Found: C, 49.05; H, 3.65%. ^{1}H NMR ($CDCl_3$, δ): 6.88 (dt, 1H, $^3J_{HH}$ = 7.9 Hz, $^4J_{PH}$ = 1.5 Hz, H5 (see atom numbering in Scheme 1)), 7.27−7.61 (m, 30H, P*Ph*$_3$), 8.35 (m, 1H, H2), 9.83 (d, 1H, $^3J_{HH}$ = 7.9 Hz, H4), 12.06 (d, 1H, $^3J_{HH}$ = 5.1 Hz, H3). ^{13}C NMR ($CDCl_3$, δ): 127.1−135.4 (m, P*Ph*$_3$ carbon resonances not individually assigned), 139.2 (t, $^3J_{PC}$ = 3.1 Hz, C5), 147.7 (t, $^3J_{PC}$ = 4.7 Hz, C2), 157.1 (t, $^2J_{PC}$ = 9.1 Hz, C4), 177.6 (t, $^2J_{PC}$ = 9.3 Hz, C3), 211.8 (t, $^2J_{PC}$ = 5.1 Hz, C1). ^{31}P NMR ($CDCl_3$, δ): −10.13 (s).

Preparation of Ir[C_3H(CH═C{Ph}S-1)(Ph-3)]Cl(PPh_3)$_2$ (4). A suspension of IrCl(CS)(PPh_3)$_2$ (0.500 g, 0.63 mmol) together with phenylacetylene (1 mL) in benzene (50 mL) was heated under reflux for 6 h to give a dark brown solution. All volatiles were removed under reduced pressure, and the residue was recrystallized from CH_2Cl_2 and heptane to give a brown solid, which was further recrystallized from CH_2Cl_2 and EtOH (twice) to give pure **4** as a green-brown, crystalline solid (0.250 g, 36%). The filtrates from these recrystallizations were combined and used for the isolation of the other isomer, compound **5** (see below). Anal. Calcd for $C_{53}H_{42}ClIrP_2S\cdot CH_2Cl_2$: C, 59.75; H, 4.09. Found: C, 59.73; H, 4.10. ^{1}H NMR ($CDCl_3$, δ): 6.84−7.68 (m, 40H, *Ph* and P*Ph*$_3$), 8.57 (t, $^3J_{PH}$ = 3.0 Hz, 1H, H4), 9.61 (s, 1H, H2). ^{13}C NMR ($CDCl_3$,

(17) Maddock, S. M.; Rickard, C. E. F.; Roper, W. R.; Wright, L. J. *Organometallics* **1996**, *15*, 1793.
(18) Lu, G.-L.; Roper, W. R.; Wright, L. J.; Clark, G. R. *J. Organomet. Chem.* **2005**, *690*, 972.
(19) Hill, A. F.; Wilton-Ely, J. D. E. T. *Inorg. Synth.* **2002**, *33*, 244.

δ): 126.1−135.0 (m, P*Ph*$_3$ and *Ph* carbon resonances not individually assigned), 139.1 (s, C5), 141.2 (t, $^3J_{PC}$ = 4.6 Hz, C2), 146.6 (s, *Ph* on C5), 151.8 (t, $^2J_{PC}$ = 10.7 Hz, C4), 157.1 (s, *Ph* on C3), 195.3 (t, $^2J_{PC}$ = 8.4 Hz, C3), 206.3 (t, $^2J_{PC}$ = 5.4 Hz, C1). ^{31}P NMR ($CDCl_3$, δ): −12.48 (s).

Preparation of Ir[C$_3$H(CH═C{Ph}S-1)(Ph-2)]Cl(PPh$_3$)$_2$ (5). The solid isolated from the combined filtrates obtained during the isolation of compound **4** (see above) was subjected to column chromatography on silica gel using CH_2Cl_2 as eluent. Three bands were observed, the first of which proved to contain complex **6** (in 5% yield, see below), the second of which was not identified, and the third brown band yielded impure **5** in very low yield (less than 5%). Because of the low yield and impure nature of this material only limited spectroscopic data were collected for this compound, but fortuitously a single crystal of compound **5**, suitable for X-ray study, was grown from CH_2Cl_2/heptane and characterization of this compound rests principally on the crystal structure obtained. ^{1}H NMR ($CDCl_3$, δ): 10.03 (s, H4), 12.78 (s, H3). ^{31}P NMR ($CDCl_3$, δ): −4.38 (s).

Preparation of Ir[η^5-C$_5$H$_2$(SCPh═CH-1)(Ph-3)(Ph-5)]Cl(PPh$_3$) (6). Ir[C$_3$H(CH═C{Ph}S-1)(Ph-3)]Cl(PPh$_3$)$_2$ (**4**; 0.100 g, 0.10 mmol) and phenylacetylene (0.110 mL, 1.00 mmol) in toluene (20 mL) were heated under reflux for 1 h to give a dark red solution. All volatiles were removed under reduced pressure, and the resulting residue was washed with hexane. The resulting solid was recrystallized from CH_2Cl_2/EtOH to give pure **6** as red crystals (0.080 g, 93%). Compound **6** could also be made directly from IrCl(CS)(PPh$_3$)$_2$ and excess phenylacetylene by heating in toluene under reflux for 1 h and using an isolation procedure similar to that described above but with an additional step involving chromatography on silica gel with a mixture of CH_2Cl_2 and hexane (1:1) as eluent. The yield by this route is approximately 50%. Crystals suitable for X-ray study were grown from CH_2Cl_2/EtOH over several days and proved to be a 1:1 CH_2Cl_2 solvate. Anal. Calcd for $C_{43}H_{33}ClIrPS\cdot CH_2Cl_2$: C, 57.11; H, 3.81. Found: C, 57.41; H, 3.97. ^{1}H NMR ($CDCl_3$, δ): 5.11 (d, $^4J_{HH}$ = 2.0 Hz, 1H, H2 or H4), 6.75−6.80 (m, 3H, *Ph* substituents), 6.99−7.43 (m, 27H, P*Ph*$_3$ and *Ph* substituents), 6.93 (d, $^4J_{HH}$ = 2.0 Hz, 1H, H2 or H4), 8.09 (d, $^3J_{PH}$ = 7.5 Hz, 1H, H6). ^{13}C NMR ($CDCl_3$, δ): 82.5 (s, CH, C2 or C4), 85.8 (d, $^2J_{PC}$ = 15.1 Hz, C1), 93.2 (s, C3 or C5), 100.6 (s, C3 or C5), 102.1 (s, CH, C2 or C4), 128.0 (d, $^2J_{PC}$ = 11.1 Hz, *o*-P*Ph*$_3$), 130.5 (s, *p*-P*Ph*$_3$), 131.3 (d, $^1J_{PC}$ = 57.3 Hz, *i*-P*Ph*$_3$), 134.3 (d, $^3J_{PC}$ = 10.1 Hz, *m*-P*Ph*$_3$), 124.8, 125.9, 126.1, 127.2, 127.6, 127.7, 128.2, 128.7, 128.8, 130.9, 132.2, 139.8 (s, carbon atoms of Ph substituents), 130.4 (s (P coupling not resolved), CH, C6), 163.3 (d, $^3J_{PC}$ = 4.0 Hz, C7). ^{31}P NMR ($CDCl_3$, δ): 1.63 (s).

Preparation of Ir[C$_3$H(CH═C{CO$_2$Me}S-1)(CO$_2$Me-2)]I(PPh$_3$)$_2$ (7). IrI(CS)(PPh$_3$)$_2$ (0.400 g, 0.45 mmol) and methyl propiolate (0.400 mL, 4.5 mmol) were added to benzene (40 mL), and the resulting suspension was stirred for 1 h at room temperature. The suspension was then heated under reflux for 5 min to give a dark brown solution. After the mixture was cooled, its volume was reduced to ca. 2 mL, and hexane (10 mL) was added to precipitate a solid. This crude product was dissolved in CH_2Cl_2 and purified by chromatography on a silica gel column (3 cm) using CH_2Cl_2 as eluent. A green band was collected and solvent removed to give a brownish green solid. This was recrystallized first from CH_2Cl_2/heptane and then from CH_2Cl_2/EtOH to give pure **2** as a dark green crystalline solid (0.258 g, 54%). The single crystal chosen for X-ray structure determination was grown from $CDCl_3$/MeOH over several days and proved to have three $CDCl_3$ molecules of solvation. Anal. Calcd for $C_{45}H_{38}IIrO_4P_2S$: C, 51.19; H, 3.63. Found: C, 51.39; H, 3.68%. IR (cm^{-1}): 1704, 1694 (CO_2Me). ^{1}H NMR ($CDCl_3$, δ): 3.53 (s, 3H, CO_2CH_3 on C2), 3.77 (s, 3H, CO_2CH_3 on C5), 7.28−7.47 (m, 30H, P*Ph*$_3$), 11.45 (s, 1H, H4), 13.23 (s, 1H, H3). ^{13}C NMR ($CDCl_3$, δ): 50.6 (s, CO_2CH_3 on C2), 52.1 (s, CO_2CH_3 on C5), 127.6 (broad, P coupling not resolved, *o*-P*Ph*$_3$), 129.6 (t′, $^{1,3}J_{PC}$ = 57.0 Hz, *i*-P*Ph*$_3$), 130.4 (s, *p*-P*Ph*$_3$), 134.9 (broad, P coupling not resolved, *m*-P*Ph*$_3$), 148.8 (s, C5), 153.5 (t, $^3J_{PC}$ = 4.5 Hz, C2), 159.1 (s, C6), 161.8 (s, C7), 177.9 (t, $^2J_{PC}$ = 8.5 Hz, C4), 198.9 (t, $^2J_{PC}$ = 10.6 Hz, C3), 214.2 (t, $^2J_{PC}$ = 4.4 Hz, C1). ^{31}P NMR ($CDCl_3$, δ): −8.75 (s).

Preparation of Ir[C$_5$H$_2$(CH═C{CO$_2$Me}S-1)(CO$_2$Me-2)(CO$_2$Me-4)]Cl(PPh$_3$)$_2$ (8). A green solution of compound **7** (0.150 g, 0.14 mmol) in THF (15 mL) was treated with AgO_3SCF_3 (0.039 g, 0.15 mmol) in THF (1.5 mL) to give a brown solution together with a pale yellow precipitate of AgI. After 1 h, methyl propiolate (0.028 mL, 0.30 mmol) was added and the resulting mixture was stirred for another 1 h to give a green solution. LiCl (0.032 g, 0.75 mmol) was added and the reaction mixture stirred for another 1 h. All volatiles were then removed under vacuum. The resulting solid was extracted with benzene and the extract filtered through Celite. The filtrate was then concentrated, and hexane was added to produce a brownish green precipitate. This was recrystallized from CH_2Cl_2/EtOH/benzene to give pure **3** as a blue-green solid (0.120 g, 82%). The elemental analysis of this sample corresponded to 1 benzene of solvation per molecule of **3**. However, the blue single crystal chosen for X-ray structure determination that was grown over several days from CH_2Cl_2/EtOH/benzene proved to contain 1.75 benzenes of solvation per molecule of **3**. Anal. Calcd for $C_{49}H_{42}ClIrO_6P_2S\cdot C_6H_6$: C, 58.63; H, 4.29. Found: C, 58.84; H, 4.34. IR (cm^{-1}): 1703, 1698, 1694 (CO_2Me). ^{1}H NMR ($CDCl_3$, δ): 3.54 (s, 3H, CO_2CH_3 on C7), 3.56 (s, 3H, CO_2CH_3 on C4), 3.60 (s, 3H, CO_2CH_3 on C2), 7.23−7.62 (m, 30H, P*Ph*$_3$), 7.63 (d, $^4J_{HH}$ = 2.4 Hz, 1H, H3), 10.70 (s, 1H, H6), 13.25 (d, $^4J_{HH}$ = 2.4 Hz, 1H, H5). ^{13}C NMR ($CDCl_3$, δ): 51.4 (broad, CO_2CH_3 on C2, C4, C7 not resolved), 124.0 (s, C2), 126.8 (s, C4), 127.6 (t′, $^{2,4}J_{PC}$ = 10.0 Hz, *o*-P*Ph*$_3$), 129.9 (t′, $^{1,3}J_{PC}$ = 58.4 Hz, *i*-P*Ph*$_3$), 130.3 (s, *p*-P*Ph*$_3$), 134.4 (t′, $^{3,5}J_{PC}$ = 10.0 Hz, *m*-P*Ph*$_3$), 143.7 (t, $^3J_{PC}$ = 2.5 Hz, C7), 161.0 (s, C10), 162.0 (s, C3), 165.3 (s, C9), 166.6 (s, C8), 198.2 (t, $^2J_{PC}$ = 11.0 Hz, C6), 247.5 (t, $^2J_{PC}$ = 7.8 Hz, C5), 252.7 (t, $^2J_{PC}$ = 2.8 Hz, C1). ^{31}P NMR ($CDCl_3$, δ): −0.34 (s).

X-ray Crystal Structure Determinations for Complexes 2−8. X-ray intensities were recorded on a Siemens SMART diffractometer with a CCD area detector using graphite-monochromated Mo Kα radiation (λ = 0.710 73 Å) between 83 and 85 K. Data were integrated and corrected for Lorentz and polarization effects using SAINT.[20] Semiempirical absorption corrections were applied on the basis of equivalent reflections using SADABS.[21] The structures were solved by direct or Patterson methods and refined by full-matrix least squares on F^2 using the programs SHELXS97[22] and SHELXL97.[23] All hydrogen atoms which have been included were located geometrically and refined using a riding model. In the structure of **2** there is a small elongation of the thermal ellipsoid of the sulfur atom and the presence nearby of peaks in the final difference map. This suggests that there may be a minor partial positional disorder between the I and CS ligands; however, no attempt was made to model this. Diagrams were produced using ORTEP3.[24]

All the crystal structures contain solvent molecules of crystallization. For complex **5**, Squeeze indicates that the crystals may also contain three disordered molecules of ethanol of solvation. Crystal data and refinement details for all structures are presented in Table 1.

(20) SAINT: Area Detector Integration Software; Siemens Analytical Instruments Inc., Madison, WI, 1995.

(21) Sheldrick, G. M. SADABS: Program for Semi-empirical Absorption Correction; University of Göttingen, Göttingen, Germany, 1997.

(22) Sheldrick, G. M. SHELXS97: Program for Crystal Structure Determination; University of Göttingen, Göttingen, Germany, 1977.

(23) Sheldrick, G. M. SHELXL97: Program for Crystal Structure Refinement; University of Göttingen, Göttingen, Germany, 1997.

(24) Burnett, M. N.; Johnson, C. K. ORTEP-III: Oak Ridge Thermal Ellipsoid Plot Program for Crystal Structure Illustrations; Report ORNL-6895; Oak Ridge National Laboratory, Oak Ridge, TN, 1996.

Acknowledgment. We thank the Marsden Fund, administered by the Royal Society of New Zealand, for granting a Postdoctoral Fellowship to G.-L.L. We also thank The University of Auckland Research Committee for partial support of this work through grants-in-aid.

Supporting Information Available: CIF files containing X-ray crystallographic data for complexes **2**−**8**. This material is available free of charge via the Internet at http://pubs.acs.org. Crystal data are also available from the Cambridge Crystallographic Data Centre (fax, +44-1223-336-033; e-mail, deposit@ccdc.cam.ac.uk; web, www: http://www.ccdc.cam.ac.uk) as Supplementary Publication Nos. CCDC 627308−627314 for **2**−**8**, respectively.

OM061066R